

Efficient Metal-Free Oxygen Reduction in Alkaline Medium on High-Surface-Area Mesoporous Nitrogen-Doped Carbons Made from Ionic Liquids and Nucleobases

Wen Yang,* Tim-Patrick Fellingner, and Markus Antonietti

Colloid Chemistry, Max Planck Institute of Colloids and Interfaces, Am Mühlenberg 1, 14476 Potsdam/Golm, Germany

Received September 7, 2010; E-mail: wen.yang@mpikg.mpg.de

Abstract: Mesoporous nitrogen-doped carbon materials with high surface areas up to $1500 \text{ m}^2 \text{ g}^{-1}$ were conveniently made by the carbonization of nucleobases dissolved in an all-organic ionic liquid (1-ethyl-3-methylimidazolium dicyanamide). Using hard templating with silica nanoparticles, this process yields high-surface-area nitrogen-doped carbon materials with nitrogen contents as high as 12 wt %, narrow mesopore size distribution of ca. 12 nm diameter, and local graphitic carbon structure. It is demonstrated that the resulting nitrogen-doped carbons show very high catalytic activity, even in the metal-free case in the oxygen reduction reaction (ORR) for fuel cells. Specifically, the as-prepared materials exhibit a low onset voltage for ORR in alkaline medium and a high methanol tolerance, compared with those of commercial 20 wt % Pt/C catalyst. We regard this as a first step toward an all-sustainable fuel cell, avoiding noble metals.

Developing catalytic materials for oxygen reduction reaction (ORR) is the current technological bottleneck for the industrial development of fuel cells.^{1–4} Up to now, the most efficient catalysts for ORR have been still platinum-based materials.³ However, these catalysts are not really feasible. On the one hand, they are characterized by a quite sluggish oxygen reduction at any pH.³ Moreover, the high cost of platinum and its limited supply will hamper any the large-scale application of such fuel cells.^{1–3} Therefore, the search for non-precious-metal as well as metal-free catalysts for ORR is one of the most active and competitive fields in chemistry.^{1–3}

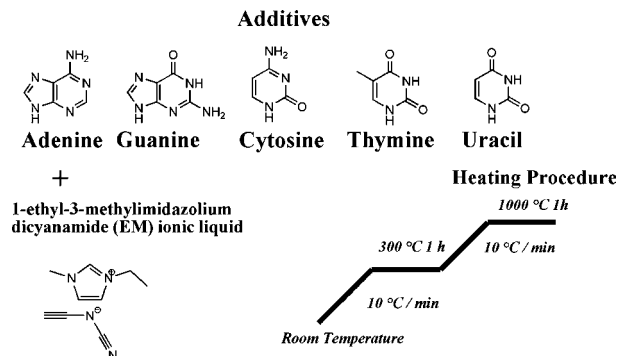
Nitrogen-doped carbons are already known to act as metal-free catalysts for oxygen reduction,^{1–3,5–16} but still on a less competitive level. It is believed that one of the limitations for enhancing the catalytic activity of these systems is the low surface density of catalytic sites,^{3,10,15} and turning to high-surface-area materials is a potential solution.^{10,15} This is what we call “mesoscopic structure control”. In addition, there is much disagreement about the nature of the active site for oxygen reduction in nitrogen-doped carbons. Some believe that transition metals may be “accidentally” incorporated during the fabricating process of the carbons materials and then play an important catalytic role during the ORR.^{2,3,5,10,16} Others propose that transition metals may not be necessary and that N-doped carbons possess inherent active sites for ORR,^{1,6–9,13} with a variety of N–C–N bonding patterns and local geometries being potentially active. This is called “microscopic structure control”. Showing ORR activity in metal-free nitrogen-doped carbon materials with high surface area is therefore at first a scientific issue, as this would prove the existence of non-metal-based ORR sites.^{1,7,13} Beside this scientific question, also the application side is of larger importance, as a noble-metal-free catalyst based on

simple carbon structures may enable fabrication of the next generation of cheap and sustainable fuel cells.

In a recent paper,¹⁷ we described the (metal-free) synthesis of nitrogen-doped carbon materials by heating nonvolatile ionic liquids featuring dicyanamide anions to temperatures of $1000 \text{ }^\circ\text{C}$. Carbons with nitrogen contents as high as 10.4%, with an electronic conductivity and oxidation stability superior to those of pure graphitic carbon, were obtained.^{17,18} This went well with the many other positive observations of improving electronic and mechanical properties of bulk carbon materials by N-doping.^{19–21} Others showed that the density of states at the Fermi level ($D(E_F)$) and the work function will increase linearly with increasing nitrogen content, creating a metal-like conductivity.^{20,21} As nitrogen also improves the HOMO position toward higher nobility,^{20,21} one might also call N-doped carbons “noble carbons” (as it compares with the effect of, e.g., chromium in noble steel).

It is the philosophy of the present contribution to gain higher nitrogen contents and microscopic structure control by incorporation of a set of natural compounds with a high atomic N/C ratio, high oxidation stability, and suitable atomic N–C–N bonding motifs that are easily available but have rarely been explored for functional carbon synthesis, namely the most familiar nucleobases, adenine (A), guanine (G), cytosine (C), thymine (T), and uracil (U) (Scheme 1). This omission of study of such bases in carbon synthesis is

Scheme 1. Precursors and Heating Procedure for N-Doped Carbon Materials



surprising, as such nucleobases can be isolated from (bacterial) biomass in larger amounts and definitely represent a sustainable raw material base for such high-performance carbons.¹² As all these nucleobases readily dissolve in the ionic liquid 1-ethyl-3-methylimidazolium dicyanamide (Emim-dca), we simply use their solutions to synthesize nitrogen-doped carbon materials by carbonization at $1000 \text{ }^\circ\text{C}$ for 1 h. As liquid and nonvolatile precursors, such educts also allow the fabrication of high-surface-area, narrowly

distributed mesoporous materials by using SiO₂ nanoparticles as hard templates for mesostructure control.^{17,22}

The resulting materials are tested in an standard ORR assay and are shown to exhibit excellent catalytic performance for the ORR and high resistance to the methanol crossover.^{1,13} It will be shown that this metal-free, sustainable system can compare favorably with commercially available Pt/C catalysts.

The nitrogen-doped carbon materials with both narrowly distributed mesoporosity and local N–C–N structural motifs were obtained from precursor mixtures of Emim-dca, nucleobase, and 12-nm SiO₂ nanoparticles. Carbonization of these initial mixtures at 1000 °C under nitrogen flow yielded carbon–silica composites. A preheating step at 300 °C was performed in order to ensure removal of water, complete dissolution of the nucleobases, and homogeneity of the final samples. After dissolution of the silica template, high-surface-area, mesoporous carbons were obtained. The materials derived from the pure ionic liquid (internal reference) and from the adenine, guanine, cytosine, thymine, and uracil solution were denoted as meso-Em, meso-EmA, meso-EmG, meso-EmC, meso-EmT, and meso-EmU, respectively. Typical transmission electron microscopy (TEM) images are shown for meso-EmG in Figure 1. The mesopore structures nicely reflect the previous

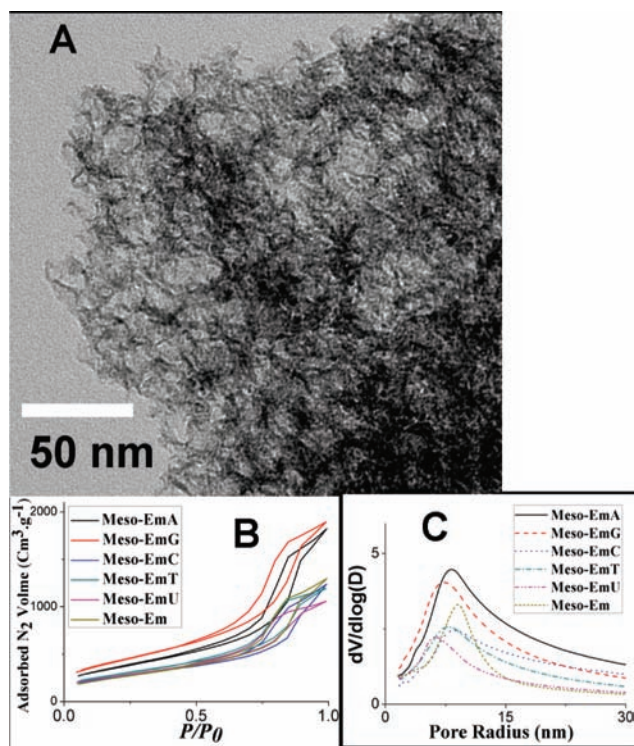


Figure 1. TEM images of meso-EmG (A). N₂ sorption isotherms (B) and pore size distribution (C) from BJH method of as-prepared high-surface-area nitrogen-doped carbon materials.

packing of silica spheres, confining the carbonization reaction. The textural properties of the resulting nitrogen-doped carbon materials were assessed by N₂ sorption and are summarized in Table S1 (Supporting Information). Gas sorption isotherms (Figure 1B) exhibit type IV curves, typical for mesoporous materials.^{13,17} Meso-EmG exhibits the highest surface area (1553 m² g⁻¹), with a total pore volume of 2.58 cm³ g⁻¹. These values rank these materials among the high surface carbons.²³ The mesopore radius distribution is centered at 7.4 nm according to the Barrett–Joyer–Halenda (BJH) model (Figure 1C), in agreement with the size of the templating silica nanoparticles.

X-ray diffraction (XRD) patterns of the resulting mesoporous nitrogen-doped carbon materials (Figure S1, Supporting Information) show two broad XRD diffraction peaks for all samples, usually attributed to the inter-plane (002) ($2\theta = 24.7^\circ$) and the inner-plane (110) ($2\theta = 43.7^\circ$) reflections of graphitic carbon.^{13,17} After introduction of nucleobase additives, the dominating (002) XRD peak shifts to slightly higher angles ($\theta = 25.1^\circ$), with a corresponding interplanar *d*-spacing (*d*₀₀₂) of 3.54 Å (as compared to *d*₀₀₂ = 3.60 Å of meso-Em). There are a number of reasons for such a compression, but at least it proves the introduction of the nucleobase additives into the graphitic body. The final composition was analyzed by elemental analysis (Table S1). In agreement with expectations, the nitrogen content increases strongly from 8.8 wt % (meso-Em) to around 12.0 wt % with the various nucleobases. This value is, to our knowledge, the highest reported value for a one-step syntheses of N-doped carbon, although 13.6 wt % could be obtained by postfunctionalization.²⁴ The molar composition of meso-Em is C₁N_{0.12}O_{0.16}H_{0.18}, while a typical composition for samples obtained with nucleobase additives is obtained for meso-EmG with C₁N_{0.15}O_{0.13}H_{0.18}. Nucleobases therefore act as efficient N-donors.

The electrocatalytic properties of the mesoporous nitrogen-doped carbon materials were evaluated for ORR using a three-electrode chemical station.^{1,13} Figure 2 depicts cyclic voltammograms (CV)

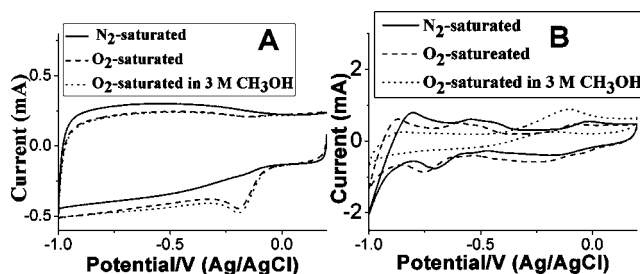


Figure 2. Cyclic voltammograms of meso-EmG (A) and commercial 20 wt % Pt/C catalyst (B) on a glassy carbon electrode in N₂-saturated 0.1 M KOH, O₂-saturated 0.1 M KOH, and O₂-saturated 0.1 M KOH and 3 M CH₃OH solutions.

for O₂ reduction on meso-EmG (A), as compared to a commercial Pt/C catalyst (B) as a reference (20 wt % platinum on carbon black). The electrolyte was a 0.1 M N₂- or O₂-saturated KOH solution. Meso-EmG (Figure 2A) does not show any significant peak in the N₂-saturated solution but does show a quasi-rectangular voltammogram, typical of high-surface-area carbons and supercapacitor performance.²⁵ In the presence of oxygen, a well-defined cathodic peak appears at -0.192 V (vs Ag/AgCl). This value is positively shifted by 68 mV in comparison with previous reports.¹³ This already indicates the excellent catalytic ability of our samples for ORR. Since typical commercial Pt/C catalysts are known to be prone to methanol poisoning, we specifically assessed the effect of methanol on ORR for both meso-EmG and commercial Pt/C. The CV scans for the commercial catalyst are shown Figure 2B. In an electrolyte saturated with O₂ and containing methanol (3 M), the cathodic peaks for oxygen reduction disappear, while one pair of peaks is observed at -0.174 and -0.110 V, which is characteristic for methanol reduction–oxidation.¹³ When investigating the behavior of meso-EmG in the same O₂-saturated methanol solution (Figure 2A), no activity specific to methanol is observed, while the characteristic peaks of ORR are maintained. These results indicate that the as-prepared mesoporous carbons can reduce oxygen but are tolerant to methanol.^{1,13} This methanol inertness goes well with chemical expectations for the catalysis of such systems.

For a potential influence of microstructure, the different nucleobase materials were studied by linear voltamperometry on a rotating disk working electrode and compared to the 20 wt % Pt/carbon sample.^{1,13} Figure 3A shows the polarization curves of the different

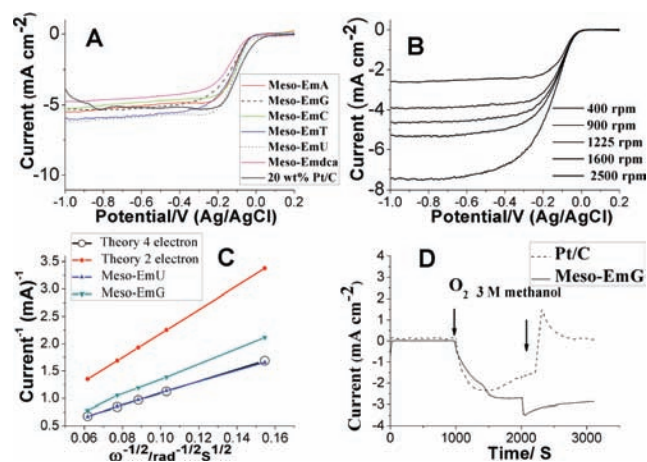


Figure 3. (A) Polarization curves on a glassy carbon rotating disk electrode for N-doped carbons, as compared with 20 wt % Pt/C in O₂-saturated 0.1 M KOH at a scan rate of 10 mV s⁻¹ and rotation rate of 1600 rpm. (B) Voltamperograms for oxygen reduction on a meso-EmG electrode in O₂-saturated 0.1 M KOH at various rotation speeds; scan rates, 10 mV s⁻¹. (C) Koutecky–Levich plot of meso-EmU at -0.35 V. Parameters used for the calculation are as follows: concentration of O₂, 1.2 × 10⁻³ mol L⁻¹; diffusion coefficient of O₂, 1.9 × 10⁻⁵ cm² s⁻¹; kinematic viscosity of the electrolyte solution, 0.01 cm² s⁻¹. (D) Current–time (*i*–*t*) response of meso-EmG and 20 wt % Pt/carbon at -0.26 V in 0.1 M KOH saturated with N₂ (0–1000 s) or O₂ (1000–2000 s) and in O₂-saturated 3 M CH₃OH (2000–3000 s).

materials in a 0.1 M O₂-saturated KOH solution. The onset potentials of oxygen reduction on the carbon materials are approximately 35 mV (Ag/AgCl), thus corresponding to an overpotential ca. 25 mV higher than the commercial Pt catalyst. Interestingly, this is rather independent of the specific nucleobase which was used and also quite similar for the pure ionic liquid-based material; i.e., the catalytically active functional site is simpler than the nucleobases as such. However, the plateau current is higher with carbons obtained from nucleobases than with the meso-Em sample, indicating a higher density of active surface sites.

Typical current–potential curves of N-doped carbons in an O₂-saturated 0.1 M KOH electrolyte are shown for meso-EmG (Figure 3B) over a range of electrode rotation rates. The current shows the typical increase with rotation rate due to the shortened diffusion layer.^{1,13} Analysis of the plateau currents through Koutecky–Levich plots (Figure 3C) reveals the reduction of O₂ with meso-EmU catalysts by a four-electron process (*n* = 4.1),²⁶ as is the case for the Pt-based catalyst, thus yielding water as the main product. For the other nucleobase-based materials, as depicted for meso-EmG, we find a slightly slower slope (*n* = 3.2), which might indicate mixed processes. Detailed experiments are, however, underway to assess this specific point.

We also investigated the electrocatalytic properties of the mesoporous nitrogen-doped carbon materials for oxygen reduction in acid electrolyte. Figure S2 (Supporting Information) shows the polarization curves for the ORR in O₂-saturated 0.1 HClO₄ on meso-EmG as an example and for commercial Pt/C catalysts. meso-EmG exhibits high catalytic activity toward ORR, with an onset potential at 0.573 V (vs Ag/AgCl) and a 197 mV overpotential as compared with Pt/C. This higher overpotential in acidic medium supports the previous view that ORR activities of nitrogen-doped carbon

materials are higher in alkaline medium than in acid medium, while the ORR activity of low-index Pt(*hkl*) single-crystal electrodes in alkaline medium is lower than the value obtained in acidic medium.^{27,28}

A methanol crossover test on meso-EmG was also performed in the chronoamperometric measurements. Figure 3D shows the corresponding response at a constant voltage of -0.26 V for 3000 s in an 0.1 M KOH solution first saturated with N₂ (0–1000 s), then gased with O₂ (1000–2000 s), and then after addition of methanol to yield an O₂-saturated 3 M CH₃OH for the 2000–3000 s period. The meso-EmG sample exhibits a strong and stable amperometric response after introduction of O₂ (1000–2000 s) into the solution, which does not suffer after introduction of methanol, suggesting a remarkably good tolerance to fuel crossover effects for nitrogen-doped carbon materials. For Pt/C, the ORR cathodic current vanishes, and an anodic current of methanol oxidation appears.

To summarize, we were able to find high ORR activity for micro- and mesoscopically structured high-surface-area nitrogen-doped carbons, with cathodic currents in the alkaline very similar to those of commercial Pt/C catalysts. In addition, the material based on a fluid, nonvolatile mixture of an ionic liquid with nucleobases is rather sustainable and cheap and can be shaped, printed, or structured before calcination, as illustrated by successful hard templating here. As a carbon-based catalyst, it also avoids typical fuel spillover sensitivities of ordinary noble metals in alkaline medium, making the engineering and construction of fuel cells more simple. This suggests that such metal-free carbon catalysts could, in principle, indeed overcome the limitations of Pt-based systems and provide suitable, sustainable, and cheap solutions for the further technological development of fuel cells and oxygen electrodes in general. Work to improve oxygen reduction in acidic media is still ongoing, and we believe that adding simple metals (as Co and Fe) to the formulation might offer further potentialities.

Acknowledgment. We thank the Max Planck Society and the ERC (Senior Excellence Grant) for supporting this project. Dr. David Portehault and Prof. Xinchun Wang are thanked for cooperation and discussion.

Supporting Information Available: Experimental details and more characterization and results. This material is available free of charge via the Internet at <http://pubs.acs.org>.

References

- Gong, K. P.; Du, F.; Xia, Z. H.; Durstock, M.; Dai, L. M. *Science* **2009**, *323*, 760.
- Lefevre, M.; Proietti, E.; Jaouen, F.; Dodelet, J. P. *Science* **2009**, *324*, 71.
- Jaouen, F.; Herranz, J.; Lefevre, M.; Dodelet, J. P.; Kramm, U. I.; Herrmann, I.; Bogdanoff, P.; Maruyama, J.; Nagaoka, T.; Garsuch, A.; Dahn, J. R.; Olson, T.; Pylypenko, S.; Atanassov, P.; Ustinov, E. A. *Appl. Mater. Interf.* **2009**, *1*, 1623.
- Zhang, M. N.; Yan, Y. M.; Gong, K. P.; Mao, L. Q.; Guo, X.; Chen, Y. *Langmuir* **2004**, *20*, 8781.
- Pylypenko, S.; Mukherjee, S.; Olson, T. S.; Atanassov, P. *Electrochim. Acta* **2008**, *53*, 7875.
- Bezerra, C. W. B.; Zhang, L.; Lee, K. C.; Liu, H. S.; Marques, A. L. B.; Marques, E. P.; Wang, H. J.; Zhang, J. J. *Electrochim. Acta* **2008**, *53*, 4937.
- Matter, P. H.; Ozkan, U. S. *Catal. Lett.* **2006**, *109*, 115.
- Nallathambi, V.; Lee, J. W.; Kumaraguru, S. P.; Wu, G.; Popov, B. N. *J. Power Sources* **2008**, *183*, 34.
- Ozaki, J.; Anahara, T.; Kimura, N.; Oya, A. *Carbon* **2006**, *44*, 3358.
- Jaouen, F.; Lefevre, M.; Dodelet, J. P.; Cai, M. *J. Phys. Chem. B* **2006**, *110*, 5553.
- Ikeda, T.; Boero, M.; Huang, S. F.; Terakura, K.; Oshima, M.; Ozaki, J. *J. Phys. Chem. C* **2008**, *112*, 14706.
- Maruyama, J.; Fukui, N.; Kawaguchi, M.; Abe, I. *J. Power Sources* **2009**, *194*, 655.
- Liu, R. L.; Wu, D. Q.; Feng, X. L.; Mullen, K. *Angew. Chem., Int. Ed.* **2010**, *49*, 2565.
- Tang, Y. F.; Allen, B. L.; Kauffman, D. R.; Star, A. *J. Am. Chem. Soc.* **2009**, *131*, 13200.

- (15) Zhang, L.; Lee, K.; Bezerra, C. W. B.; Zhang, J. L.; Zhang, J. J. *Electrochim. Acta* **2009**, *54*, 6631.
- (16) Cote, R.; Lalande, G.; Guay, D.; Dodelet, J. P.; Denes, G. *J. Electrochem. Soc.* **1998**, *145*, 2411.
- (17) Paraknowitsch, J. P.; Zhang, J.; Su, D. S.; Thomas, A.; Antonietti, M. *Adv. Mater.* **2010**, *22*, 87.
- (18) Lee, J. S.; Wang, X. Q.; Luo, H. M.; Baker, G. A.; Dai, S. *J. Am. Chem. Soc.* **2009**, *131*, 4596.
- (19) Kim, D. P.; Lin, C. L.; Mihalisin, T.; Heiney, P.; Labes, M. M. *Chem. Mater.* **1991**, *3*, 686.
- (20) Czerw, R.; Terrones, M.; Charlier, J. C.; Blase, X.; Foley, B.; Kamalakaran, R.; Grobert, N.; Terrones, H.; Tekleab, D.; Ajayan, P. M.; Blau, W.; Ruhle, M.; Carroll, D. L. *Nano Lett.* **2001**, *1*, 457.
- (21) Carvalho, A. C. M.; Dos Santos, M. C. *J. Appl. Phys.* **2006**, *100*, 084305.
- (22) Portehault, D.; Giordano, C.; Gervais, C.; Senkowska, I.; Kaskel, S.; Sanchez, C.; Antonietti, M. *Adv. Funct. Mater.* **2010**, *20*, 1827.
- (23) Kim, W.; Joo, J. B.; Kim, N.; Oh, S.; Kim, P.; Yi, J. H. *Carbon* **2009**, *47*, 1407.
- (24) Hulicova-Jurcakova, D.; Kodama, M.; Shiraishi, S.; Hatori, H.; Zhu, Z. H.; Lu, G. Q. *Adv. Funct. Mater.* **2009**, *19*, 1800.
- (25) Simon, P.; Gogotsi, Y. *Nat. Mater.* **2008**, *7*, 845.
- (26) Wroblowa, H. S.; Pan, Y. C.; Razum Tney, G. *J. Electroanal. Chem.* **1976**, *69*, 195.
- (27) Piana, M.; Catanorchi, S.; Gasteiger, H. A. *ECS Trans.* **2008**, *16*, 2045.
- (28) Meng, H.; Jaouen, F.; Proietti, E.; Lefevre, M.; Dodelet, J. P. *Electrochem. Commun.* **2009**, *11*, 1986.

JA108039J